Quantitation of Function: Relative Measurements

8

Introduction

Essentially all diagnostic nuclear medicine studies are made up of a series of images. Interpretation of most of these studies involves visual assessment of the biodistribution of a radiopharmaceutical as depicted in the images without any numeric quantification, e.g., Bone Imaging Study with Tc-99m-MDP. In fact, the eye-brain complex is moderately accurate in estimating the relative amounts of radiopharmaceutical within various structures in images. And visual inspection can identify and compensate for overlap of structures and artifacts better than quantitative results generated from regions of interest (ROIs).

However, in a significant number of diagnostic nuclear medicine procedures, it is useful to quantitate one or more functional parameters such as myocardial perfusion in the Myocardial Perfusion Study with Tc-99m-sestamibi. The quantitative measurement can be in either relative or absolute terms. When the quantitative measurement is in relative terms, either it compares the amount of activity in one area to the amount of activity in another area, often in the same image, or it compares the activity in the same structure in multiple images acquired at different points in time. Table 8.1 lists those studies that typically include quantitative measurements of function in relative terms.

In contrast, a quantitative measurement is in absolute terms when the amount of activity in an area or structure of interest within an image is compared to the amount of activity that was injected. The evaluation may end with the percent uptake in the structure in question, e.g., Thyroid Uptake Measurement with I-123, or the percent uptake may be converted to a physiologic parameter, e.g., renal clearance in terms of effective renal plasma flow (ERPF) in the Renal Tubular Secretion Study with Tc-99m-MAG3. Absolute measurements are discussed in Chap. 9, Quantitation of Function: Absolute Measurements.

Relative quantitative measurements require techniques or strategies that compensate or correct for (1) attenuation of photons that are emitted from the structure

W.C. Klingensmith III, *The Mathematics and Biology of the Biodistribution of Radiopharmaceuticals-A Clinical Perspective*,
DOI 10.1007/978-3-319-26704-3_8

Table 8.1 Nuclear medicine studies that involve the measurement of relative activity

Procedure	Radiopharmaceutical	Functional parameter	Image type	Attenuation correction	Background subtraction
Cardiovascular system					
Cardiac Gated Blood Pool Study	Tc-99m-red blood cells	Ejection fraction	Planar	No	Background ROI
Myocardial Perfusion Study	N-13-ammonia	Myocardial perfusion (clearance)	PET-CT	CT density map	Tomography
Myocardial Perfusion Study	Rb-82 as rubidium chloride	Myocardial perfusion (clearance)	PET-CT	CT density map	Tomography
Myocardial Perfusion Study	Tc-99m-sestamibi	Myocardial perfusion (clearance)	SPECT(-CT)	Comparison to normal range	Tomography
Myocardial Perfusion Study	Tl-201 as thallous chloride	Myocardial perfusion (clearance) Myocardial viability (equilibrium)	SPECT(-CT)	Comparison to normal range	Tomography
Myocardial Viability Study	F-18-FDG	Myocardial viability (clearance)	PET-CT	CT density map	Tomography
Central nervous system					
Ventricular Shunt Study	Tc-99m-DTPA	Washout time	Planar	No	No background activity
Gastrointestinal system					
Esophageal Motility Study	Tc-99m-sulfur colloid	Transit time	Planar	No (?)	No background activity
Gastric Emptying Study	Tc-99m-sulfur colloid	Transit time	Planar	Geometric mean of opposing images	No background activity
Hepatic Artery Perfusion Study	Tc-99m-MAA	Hepatic artery perfusion (clearance)	Planar	Geometric mean of opposing images	No background activity
Hepatobiliary Study	Tc-99m-trimethylbromo-IDA	Gallbladder ejection fraction	Planar	No	Background ROI
Genitourinary system					
Renal Glomerular Filtration Study	Tc-99m-DTPA	Half time of peak cortical activity	Planar	No	Background ROI
Renal Tubular Excretion Study	Tc-99m-MAG3	Half time of peak cortical activity	Planar	No	Background ROI
Renal Tubular Function Study	Tc-99m-DMSA	Clearance	Planar	No	Background ROI

of interest in the direction of the imaging machine or probe but are deflected or absorbed in the intervening tissue and (2) extraneous photons from radioactivity that is outside of the structure of interest but within the field of view of the imaging machine or probe. The issue of limited geometry of the field of view of the imaging machine is not a problem in relative measurements because the field of view is the same in all images. This is also true for factors such as infiltration of an intravenously injected radiopharmaceutical, which will decrease the delivery of tracer to all tissues because the decrease will be the same everywhere and cancel for relative measurements.

Quantitative Measurement of Relative Function: Overview

In Table 8.1 under "Attenuation correction," no explicit attenuation correction is performed in many planar studies in which multiple measurements are made in the same location over time. It is assumed that there is relatively little change in attenuation over time, and since one time point is compared to another, attenuation implicitly cancels. In the case of SPECT images, it is assumed that the tomographic reconstruction is sufficient to minimize the effect of attenuation so that activity in one location can be compared to another location at the same point in time.

In the case of PET-CT, there is relatively accurate attenuation correction inherent in the PET images because both the PET and CT images are tomographic and have essentially uniform spatial resolution across the field of view, and the CT images are density maps that correlate with the spatial distribution of attenuation so that they can be used to correct the PET images for photon attenuation.

The geometric mean method of relative attenuation correction is used for the Gastric Emptying Study and the Hepatic Artery Perfusion Study because the structures of interest vary in their distance to the anterior and posterior body surfaces in a given patient. The mathematic explanation for why the geometric mean corrects for relative attenuation when the activity varies in its distance to the anterior and posterior body surfaces is presented below.

In Table 8.1 under "Background subtraction," it can be seen that those studies that generate tomographic images or in which the radiopharmaceutical is confined to the structure of interest, e.g., Ventricular Shunt Study and Gastric Emptying Study, no background subtraction is needed. This leaves the Cardiac Gated Blood Pool Study with Tc-99m-RBCs, the Hepatobiliary Study with Tc-99m-trimethylbromo-IDA, and the three renal studies as studies that benefit from background subtraction. The formula for performing background subtraction is discussed below.

The issue of detection geometry varies among imaging modalities and studies, but since it is the same within a study for all images and since the measurements are all relative, the effect of detection geometry occurs in both the numerator and denominator and cancels. Therefore, no adjustment needs to be made to compensate for suboptimal detection geometries in relative quantification.

Quantitative Measurement of Relative Function: Attenuation Correction

Uniform Attenuation The equation for attenuation of a beam of photons passing through tissue is

$$A(\text{cps}) = A_0(\text{cps})e^{\mu x} \tag{8.1}$$

where A is the detected activity or intensity of photons in terms of counts per second, A_0 is the original activity in terms of counts per second, μ is the linear attenuation coefficient with units of 1/cm, x is the length of tissue that the photons pass through in centimeters, and e is the natural log. The parameter μ varies with the density of the tissue and the energy of the photons.

Figure 8.1 shows a diagram of a cross section of the abdomen at the level of the kidneys with a gamma camera positioned posteriorly. The broken lines indicate the tissue that photons that originate in the kidneys need to pass through on their way to the gamma camera. There will also be some attenuation of photons by renal tissue, self-absorption. In the three renal studies, the anatomy of the kidneys and the thickness and density of the tissue between the kidneys and gamma camera are assumed to be quite symmetrical. (*A* somewhat more refined approach is used when correcting renal counts in the Renal Tubular Secretion Study with Tc-99m-MAG3 in order to determine the absolute clearance as effective renal plasma flow (ERPF)) Thus, for relative measurements, e.g., left and right, the number of counts recorded from ROIs placed over the right and left kidneys can be compared by dividing one by the other:

$$\frac{A_L(\text{cps})}{A_R(\text{cps})} = \frac{A_{0L}e^{-\mu x}(\text{cps})}{A_{0R}e^{-\mu x}(\text{cps})} \tag{8.2}$$

The factors relating to attenuation, i.e., the density of the tissue and the length of the pathway through the tissue will be essentially the same on the two sides and cancel:

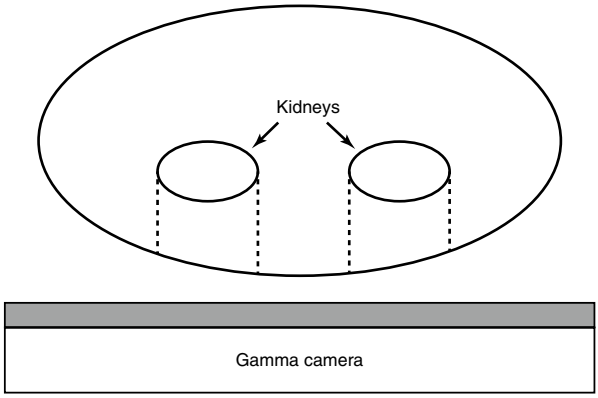

Fig. 8.1 Diagram of abdominal cross section through the kidneys. There is a single gamma camera (collimator in *gray*) posterior to the patient. The *broken lines* enclose tissue that will attenuate gamma rays that originate from renal activity. There will also be some attenuation of gamma rays by the renal tissue itself (self-absorption)

$$\frac{A_{\mathrm{L}}\,(\mathrm{cps})}{A_{\mathrm{R}}\,(\mathrm{cps})} = \frac{A_{0\mathrm{L}}\,(\mathrm{cps})}{A_{0\mathrm{R}}\,(\mathrm{cps})} \tag{8.3}$$

Thus, the ratio of counts in the ROIs over the left and right kidneys in the images will reflect the ratio of the actual amount of radiopharmaceutical in the left and right kidneys.

Use of the Geometric Mean In studies like the Gastric Emptying Study with Tc-99m-sulfur colloid-labeled oatmeal, multiple images are acquired over time as the radiopharmaceutical passes through the stomach. However, the successive components of the stomach, fundus, body, and antrum, are at different distances from the anterior and posterior skin surfaces (Fig. 8.2).

The arrows indicate the movement of radiopharmaceutical from the posterior fundus to the more anteriorly placed body and then to the anteriorly placed antrum. These three tomograms of the stomach would normally be in three different images from cephalad to caudad levels in the abdomen.

Thus, for the number of counts in different portions of the stomach to be comparable in either the anterior or posterior image alone, there needs to be a form of attenuation correction that takes into account the varying distance of the stomach components from the posterior and anterior skin surfaces. This is not possible without knowing the distance of the various stomach components to the skin. However, by acquiring simultaneous anterior and posterior images over time, identical ROIs

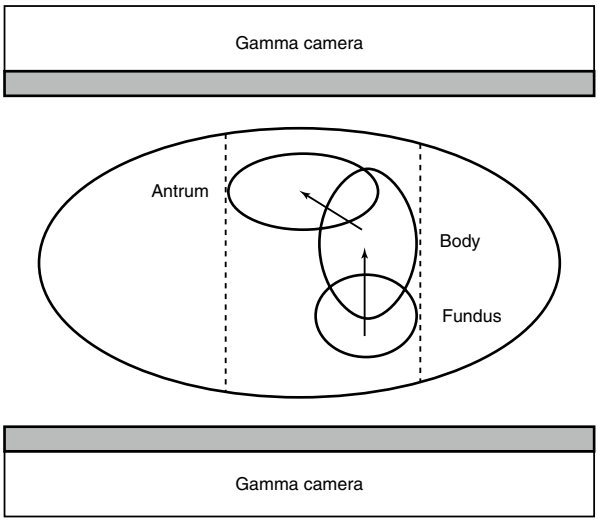

Fig. 8.2 Dual-headed gamma camera. Dual opposed gamma cameras are positioned anterior and posterior to the upper abdomen in a Gastric Emptying Study. Three images through the fundus, body, and antrum are superimposed to demonstrate that the position of a test meal varies in the anteroposterior direction as it passes through the stomach. Quantitating the data with the geometric mean approach compensates for this variable

can be placed over the stomach in both the anterior and posterior images, the counts can be measured at multiple time points, and then the geometric mean can be calculated for each time point.

The geometric mean, in general, is the *n*th root of the product of *n* numbers. In the case of anterior and posterior images, it is the second (square) root of the anterior and posterior ROI counts multiplied together. If the total distance from anterior skin to posterior skin is taken to be *d* and the distance from the anterior skin to the stomach lumen is *x* then the distance from the posterior skin to the stomach lumen will be $d-x$, giving,

$$A_{\mathrm{GM}}\left(\mathrm{cts}\right)=\left[A_0e^{-\mu x}\left(\mathrm{cts}\right)\ A_0e^{-\mu(d-x)}\left(\mathrm{cts}\right)\right]^{1/2} \tag{8.4}$$

where A_{GM} is the geometric mean of the activity in the stomach as determined from the anterior and posterior images, A_0 (cts) $e^{-\mu x}$ is the counts recorded from the anterior gastric region of interest, and A_0 (cts) $e^{-\mu(I-x)}$ is the counts recorded from the posterior region of interest. The right-hand side of Eq. 8.4 can be simplified,

$$\left[A_0\ e^{-\mu x}\left(\mathrm{cts}\right)\ A_0\ e^{-\mu(d-x)}\left(\mathrm{cts}\right)\right]^{1/2}=\left[A_0^2\ e^{-\mu d}\right]^{1/2}\left(\mathrm{cts}\right)=A_0e^{-\mu d/2}\left(\mathrm{cts}\right) \tag{8.5}$$

Notice that the distances from the anterior and posterior skin surfaces in the exponents add to *d* and, therefore, do not affect the result. Thus, the geometric mean is independent of the location of the activity in the anteroposterior dimension.

We can then make a relative comparison of the activity remaining in the stomach at any subsequent time compared to the initial activity in the stomach with additional simplification of the equation (the different times are indicated by subscripts "1" and "2"),

$$\frac{A_{\mathrm{GM2}}\left(\mathrm{cts}\right)}{A_{\mathrm{GM1}}\left(\mathrm{cts}\right)}=\frac{A_{02}e^{-\mu d/2}\left(\mathrm{cts}\right)}{A_{01}e^{-\mu d/2}\left(\mathrm{cts}\right)}=\frac{A_{02}\left(\mathrm{cts}\right)}{A_{01}\left(\mathrm{cts}\right)} \tag{8.6}$$

Normal criteria can then be established for the fraction or percent of the initial meal remaining in the stomach at one or more times after ingestion of the meal [1, 2]. As an example, a worksheet for calculating the time-activity curve for gastric emptying is included at the end of this chapter.

Comparison to a Normal Range Another method of dealing with attenuation is to perform no attenuation correction (planar images) or incomplete attenuation correction (SPECT) and to instead compare the quantitative data to a normal range that accounts for variable, but relatively reproducible, attenuation as a function of location. An example of this approach is the evaluation of myocardial perfusion with single-photon radiopharmaceuticals, e.g., Myocardial Perfusion Study with T-99m-sestamibi [3]. The apparent distribution of myocardial perfusion in the images of the left ventricle is a function of normal variation, e.g., decreased myocardium in the apex, and attenuation from differing amounts and densities of tissue between myocardium and the gamma camera. Attenuation also varies with gender, e.g., breast attenuation, so that breast size must be taken into account for females.

Quantitative Measurement of Relative Function: Background Correction

The issue of activity outside of the organ of interest contributing counts to the ROI placed over the organ of interest falls into three categories: (1) no activity outside of the organ of interest, (2) planar imaging with activity behind and in front of the organ of interest, and (3) tomography (SPECT or PET) (Table 8.1).

If the radiopharmaceutical is confined to the organ or structure of interest, e.g., Gastric Emptying Study with Tc-99m-sulfur colloid oatmeal, then there is essentially no activity in other structures and no need for background correction. Four studies in Table 8.1 fall into this category. However, if there is a significant amount of activity in the tissues around the organ of interest and planar imaging is used, then there will be unwanted counts in the ROI, e.g., Renal Tubular Secretion Study with Tc-99m-MAG3 (Fig. 8.3). Five studies in Table 8.1 are in this category.

Typically, correction for background counts is performed by placing a so-called "background" ROI, ~*B*, adjacent to the organ of interest, *K*, in a location that is expected to contain an amount of activity that is similar to the amount anterior and posterior to the organ of interest, region *B* (Fig. 8.4).

Then the average counts per pixel in the background ROI are subtracted from each of the pixels in the ROI over the organ in question.

$$K_{\mathrm{C}}(\mathrm{cts}) = \left[\left(K(\mathrm{cts}) + B(\mathrm{cts})\right) / P_{\mathrm{K}}(\mathrm{px}) - {\sim}B(\mathrm{cts}) / P_{{\sim}\mathrm{B}}(\mathrm{px})\right] P_{\mathrm{K}}(\mathrm{px}) \quad (8.7)$$

Here K_{C} is background corrected counts from a kidney ROI; $K+B$ is the number of counts in the kidney ROI, kidney + background; P_{K} is the number of pixels (px) in the kidney ROI; and $P_{\sim\mathrm{B}}$ is the number of pixels in the background ROI.

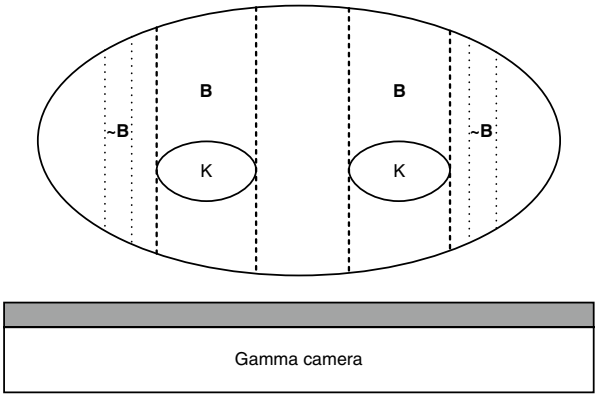

Fig. 8.3 Diagram of an abdominal cross section through the kidneys. There is a single gamma camera (collimator in *gray*) posterior to the patient. The *broken lines* enclose extrarenal tissue, *B*, that is included in the renal ROI and will contribute unwanted counts to the measurement of activity in the kidneys, *K*. An imprecise correction for background activity can be made by measuring the counts in a ROI, ~*B*, that is placed over tissue that contains approximately the same amount of activity as the background tissue anterior and posterior to the organ of interest

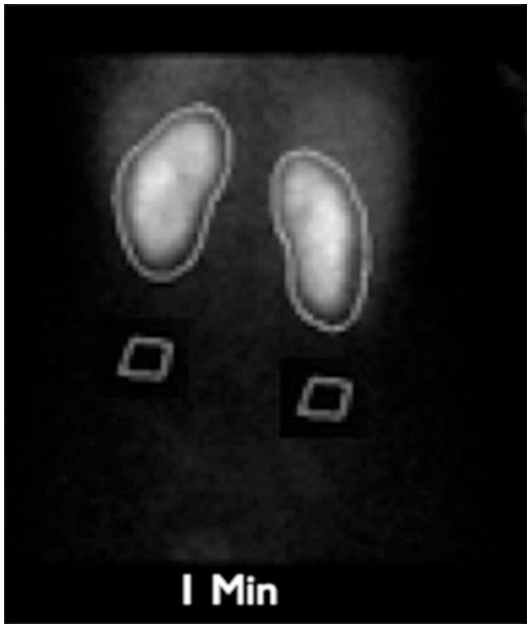

Fig. 8.4 Posterior planar 1 min image from a renal tubular secretion study. The image shows ROIs placed around the kidneys and just below the kidneys for use in background subtraction

In addition, there are another five studies in Table 8.1 in which there is activity outside of the organ of interest, but imaging is done tomographically with either SPECT-CT or PET-CT, which essentially eliminates the issue of activity outside of the organ of interest contributing counts to the ROI of the organ of interest. Over time as more and more nuclear medicine studies are performed with tomography, particularly PET-CT, fewer studies will need post image processing correction for background activity.

Quantitative Measurement of Relative Function: Relative Clearance of Two Kidneys

In the Renal Tubular Secretion Study (Tc-99m-MAG3) and Renal Glomerular Filtration Study (Tc-99m-DTPA), renal clearance is quantitated in both absolute and relative terms. For the relative quantitative measurement, the clearance of each kidney is compared to the total. First, the counts in the renal ROIs for each kidney are corrected for background activity as discussed above. Then, the percent of total renal clearance in each kidney can be calculated from the simple equation,

$$\mathrm{RK}_{\mathrm{Cl}}(\%) = \frac{\mathrm{RK}(\mathrm{cpm})}{\mathrm{RK}(\mathrm{cpm}) + \mathrm{LK}(\mathrm{cpm})} \times 100(\%) \tag{8.8}$$

where $\mathrm{RK}_{\mathrm{Cl}}$ (%) is the percent clearance of the right kidney and RK (cpm) and LK (cpm) are background corrected counts per minute for the right and left kidneys. The percent clearance of the left kidney is calculated in the same fashion.

Note that the clearance of each kidney is related to the total clearance of both kidneys in percent terms and that the clearance or uptake of tracer in the kidneys at a given time is not related to the amount of tracer administered and, therefore, is not in absolute terms and cannot be expressed in standard units of milliliters per minute (mL/min).

Gastric Emptying Worksheet

GASTRIC EMPTYING WORKSHEET

Nuclear Medicine Department

Institution_____

Name_____ ID_____ Age_____ Sex_____

Referring physician_____ Date_____

TECHNOLOGIST TO COMPLETE

Is the patient a diabetic? Yes___ No___

Has the patient had any gastrointestinal surgery? Yes___ No___

If so, describe _____

Does the patient take any medications to stimulate gastric emptying? Yes___ No___

If so, which _____

NOTE: Many nuclear medicine computers have software that performs one or more of the steps below automatically.

IMAGE ANALYSIS

STEP 1 Determine cpm/gastric ROI in all images and correct for radioactive decay:

Time to begin imaging	Time post ingestion	cpm/gastric ROI	Decay correction factor	Corrected cpm/ gastric ROI
	0 min ANT	_____	1.00	_____
_____	0 min POST	_____	1.00	_____
	15 min ANT	_____	1.03	_____
_____	15 min POST	_____	1.03	_____
	30 min ANT	_____	1.06	_____
_____	30 min POST	_____	1.06	_____
	45 min ANT	_____	1.09	_____
_____	45 min POST	_____	1.09	_____
	60 min ANT	_____	1.12	_____
_____	60 min POST	_____	1.12	_____

STEP 2 Correct for attenuation:

Time	ANT Corrected cpm/ gastric ROI		POST Corrected cpm/ gastric ROI		Product		Square root
0 min	_____	x	_____	=	_____	√	_____
15 min	_____	x	_____	=	_____	√	_____
30 min	_____	x	_____	=	_____	√	_____
45 min	_____	x	_____	=	_____	√	_____
60 min	_____	x	_____	=	_____	√	_____

STEP 3 Plot the square root results on the Gastric Emptying Study graph.

STEP 4 Compare the half time of gastric emptying to the normal range for age (same values for males & females) [1].

Age	Normal range	Reproducibility
20-40 yr	10-60 min	≤ 30 min
40-60 yr	10-40 min	≤ 20 min
60-80 yr	10-30 min	≤ 15 min

Technologist _____

References

1. Klingensmith WC, Rhea KL, Wainwright EA, et al. The gastric emptying study with oatmeal: normal range and reproducibility as a function of age and sex. J Nucl Med Technol. 2010;38:186–90.
2. Abell TL, Camilleri M, Donohoe K, et al. Consensus recommendations for gastric emptying scintigraphy:a joint report of the American Neurogastroenterology and Motility Society and the Society of Nuclear Medicine. Am J Gastroenterol. 2008;103:753–63; J Nucl Med Technol. 2008;36:44–54.
3. Widding A, Hesse B, Gadsboll N. Technetium-99m sestamibi and tetrofosmin myocardial single-photon emission tomography: can we use the same reference data base? Eur J Nucl Med. 1997;24:42–5.